Journal of Marine Science and Technology

Volume 23 | Issue 5 Article 5

DESIGN AND OPERATION OF AN EDGE-WALL SLOTTED WAVEGUIDE ARRAY ANTENNA WITH ULTRALOW SIDE LOBES FOR APPLICATION OF OFF-SHORE RADAR

Ke-Ru Chou
Department of Electrical Engineering, National Taiwan Ocean University, Keelung, Taiwan, R.O.C.

Han-Nien Lin
Department of Communications Engineering, IC-EMC Research and Development Center, Feng-Chia University, Taichung, Taiwan, R.O.C.

Wei-Hsien Lu
Green Energy and Environment Research Laboratories, Industrial Technology Research Institute (ITRI), Hsinchu, Taiwan, R.O.C.

Heng-Wen Chang
Green Energy and Environment Research Laboratories, Industrial Technology Research Institute (ITRI), Hsinchu, Taiwan, R.O.C.

Kwong-Kau Tiong
Department of Electrical Engineering, National Taiwan Ocean University, Keelung, Taiwan, R.O.C. Department of Communications, Navigation and Control Engineering, National Taiwan Ocean University, Keelung, Taiwan, R.O.C., b0114@ntou.edu.tw

Recommended Citation

Chou, Ke-Ru; Lin, Han-Nien; Lu, Wei-Hsien; Chang, Heng-Wen; and Tiong, Kwong-Kau (2015) "DESIGN AND OPERATION OF AN EDGE-WALL SLOTTED WAVEGUIDE ARRAY ANTENNA WITH ULTRALOW SIDE LOBES FOR APPLICATION OF OFF-SHORE RADAR," *Journal of Marine Science and Technology*: Vol. 23: Iss. 5, Article 5.
DOI: 10.6119/JMST-015-0226-2
Available at: https://jmstt.ntou.edu.tw/journal/vol23/iss5/5

DESIGN AND OPERATION OF AN EDGE-WALL SLOTTED WAVEGUIDE ARRAY ANTENNA WITH ULTRALOW SIDE LOBES FOR APPLICATION OF OFF-SHORE RADAR

Acknowledgements

The authors would like to thank Green Energy and Environment Research laboratories, Industrial Technology Research Institute (ITRI) for partial financial support in carrying out this research.

Journal of Marine Science and Technology, Vol. 23, No. 5, pp. 620-627 (2015)
DOI: 10.6119/JMST-015-0226-2

DESIGN AND OPERATION OF AN EDGE-WALL SLOTTED WAVEGUIDE ARRAY ANTENNA WITH ULTRALOW SIDE LOBES FOR APPLICATION OF OFF-SHORE RADAR

Ke-Ru Chou[1], Han-Nien Lin[2], Wei-Hsien Lu[3], Heng-Wen Chang[3], and Kwong-Kau Tiong[1, 4]

Key words: array antennas, edge-slotted waveguide, slot arrays, waveguide antennas, resonant shunt slots.

ABSTRACT

This paper presents the design, fabrication, and operation of an edge-wall slotted waveguide array antenna with metal flare for the generation of ultralow side lobes fan-beam radiation. The single traveling wave array antenna consists of 71 radiating elements. The radiation pattern at the operating band was designed utilizing the Taylor's aperture distribution to achieve an ultralow side lobe level (SLL) of -33 dB. The mathematical relationship between the slot characteristics and the conductance is evaluated by the least squared quadratic curve fitting procedure. Finite element method software is used to analyze the various antenna characteristics of the radiating slots, including return loss, insertion loss, and radiation patterns. The array antenna was fabricated and the performance characteristics of the antenna were measured in an antenna near-field measurement chamber. The well match of the measured and simulated results indicated the excellent design of the array antenna with ultralow side lobes. Finally, the unit was fitted onto a search radar system and an experimental test on the radar returns on Keelung Islet was carried out. The clear radar signals of the islet showed the well design of the unit.

Paper submitted 10/20/14; revised 01/29/15; accepted 02/26/15. Author for correspondence: Kwong-Kau Tiong (e-mail: b0114@ntou.edu.tw).
[1] Department of Electrical Engineering, National Taiwan Ocean University, Keelung, Taiwan, R.O.C.
[2] Department of Communications Engineering, IC-EMC Research and Development Center, Feng-Chia University, Taichung, Taiwan, R.O.C.
[3] Green Energy and Environment Research Laboratories, Industrial Technology Research Institute (ITRI), Hsinchu, Taiwan, R.O.C.
[4] Department of Communications, Navigation and Control Engineering, National Taiwan Ocean University, Keelung, Taiwan, R.O.C.

I. INTRODUCTION

Edge-wall slotted waveguide array antennas were originally developed for scientific and military researches (Emmet et al., 1972; Skolnik, 2001; Balanis, 2005). The many advantages such as, high gain, low SLL, small aperture blockage, high power handling capacity, easy manufacturing process and control of the aperture distribution, have facilitated the extensive use of edge-wall slot array antennas in many radar systems. In particular, the ability to achieve low SLL can be exploited in the design of the array antenna in coastal surveillance radar or marine radar for operation in the vicinity of or within an offshore wind farm. The existence of non-negligible SLL in close proximity of strong reflecting objects, *viz.* the wind turbine towers, may generate spurious echoes in directions other than the main beam of the radar (Brown and Howard, 2004; Matthews et al., 2009). The echoes may affect the detection of small target, e.g. fishing vessels operating in the vicinity of wind farm or even interfered with rescue operation in such location. The implementation of ultralow SLL feature in the array antenna should benefit the mitigation of the impact of wind farm on the marine radar system.

The inclined slots in the edge-wall will interrupt the flow of current and couple the power from the waveguide modal fields into radiation field in free space. The larger the inclined angle of the slot, the more abrupt will be the interruption of the surface current and leading to a larger radiation power. In order to have good control of the radiation field of a linear slot array, the waveguide should operate in single mode. Under the single mode operation at the dominant TE_{10} mode (Ramo et al., 1984), the currents $\hat{J}_s$ along the wall surfaces of the waveguide are proportional to $\hat{H}$ as shown in Fig. 1 and can be written as:

$$\hat{J}_s = \tilde{n} \times \hat{H}\Big|_{y=0} = -\hat{a}_x j \frac{A_{10}}{\omega\mu\varepsilon}\left(\frac{\pi}{a}\right)^2 \cos\left(\frac{\pi}{a}x\right)\exp(-j\beta_z z) - \hat{a}_z \frac{\beta_z A_{10}}{\omega\mu\varepsilon}\frac{\pi}{a}\sin\left(\frac{\pi}{a}x\right)\exp(-j\beta_z z) \quad (1)$$

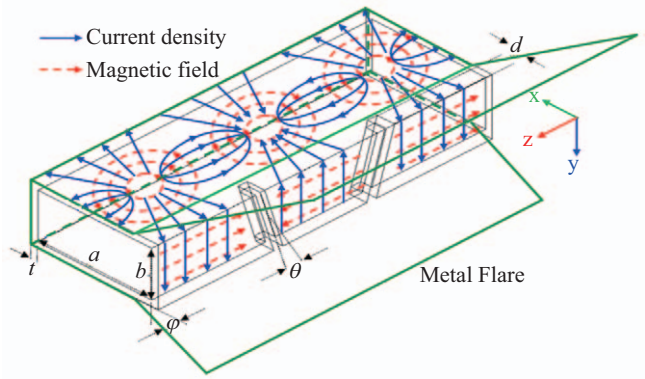

Fig. 1. Magnetic field and surface current density distribution patterns for the TE_{10} mode in a rectangular waveguide.

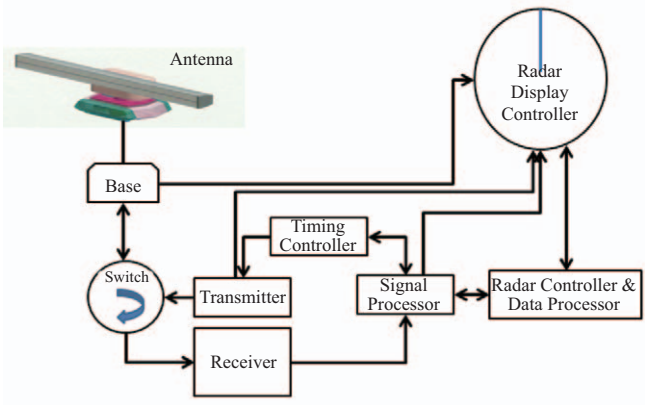

Fig. 2. Block diagram of the off-shore radar system.

and

$$\hat{J}_s = \tilde{n} \times \hat{H}\Big|_{x=0} = \hat{a}_y j \frac{A_{10}}{\omega\mu\varepsilon}\left(\frac{\pi}{a}\right)^2 \exp(-j\beta_z z) \qquad (2)$$

In (1) and (2), $\hat{J}_s$ is the surface current density, $\tilde{n}$ is the outward unit normal to the rectangular waveguide surface, $\hat{H}$ is the magnetic field intensity of the dominant TE_{10} mode, ω is the angular frequency, μ is the magnetic permeability of the medium, β is the phase constant, ε is the dielectric permittivity of the medium and a is the width of the rectangular waveguide.

The initial design considerations of the radiating slots for achieving ultralow SLL are of great concern. It is important that the radiating slots should have a proper radiated power distribution along the array since this will adversely affect the performance of the radiator. With the required power distribution, the radiation conductance values may change with the position of each radiating slot. The corresponding distribution of the radiated power depends on both the resonant length and inclined angle of the individual slot. Each radiating element of the waveguide array antenna has been constructed using longitudinal slots of shunt type with the radiating slots cut in the edge-wall of a rectangular waveguide giving horizontal polarization for the radiating fields. The usage of edge-shunt slots may lead to non-negligible cross polarization in the radiated field. This issue may be alleviated by an insertion of a suppressor consisting of a strip grating in front of the antenna array (Ando et al., 2006). The presently constructed edge-wall slotted waveguide array antenna has dimensions of 1800 mm × 150 mm × 150 mm, including the metal flare and the feed network. The array consists of seventy one regularly spaced inclined slots along the edge wall of a rectangular guide. Each excitation element has a width of 1.8 mm and a resonant length l_{res}. The resonant length l_{res} is being defined along the outer surface of the slot region and can be written as (3):

$$l_{res} = \frac{b + 2t}{\cos\theta} + 2d \qquad (3)$$

where t is the waveguide wall thickness, θ is the slot inclined angle, b is the dimension of the rectangular waveguide edge wall and d is the slot depth across the broad side of the guide. The relative orientation of the current distribution with respect to the slot angle for the TE_{10} mode in the rectangular waveguide with metal flare is being illustrated in Fig. 1.

Finite element method software is used to analyze the various antenna characteristics of the radiating slots, including return loss, insertion loss and radiation patterns. The array antenna was then fabricated and tested. The performance characteristics of the antenna were measured in an antenna near-field measurement chamber (Yaghjian, 1986). The measured and simulated results were presented and discussed.

In order to verify the well performance of the radiator unit, an off-shore search radar system was set up with the fabricated unit operates as the radiator. The schematic block diagram of the assembled radar system is illustrated in Fig. 2. The radar system must contain at least several basic elements. These are a base, a transmitter, an antenna, a receiver, a switcher, a signal processor and an indicator. The base includes a motor, gear system, and slipping ring. The transmitter produces a radio frequency signal which is delivered to the antenna to be beamed toward the target. A portion of the transmitted electromagnetic wave is scattered by the target in the direction of the receiving antenna, where it is collected and delivered to the receiver. The time control diagram generates the synchronization timing signals required throughout the system. Switching the antenna between the transmitting and receiving signals is controlled by the switcher. The switcher allows the same antenna to be used both as transmitter and receiver. The signal processor calculated the intermediate frequency signal and controlled the turning speed of the base. The display controller offer the man-machine interface of the system and display the return echo information on the screen. The display conveys target information to the radar operator. In the experimental test, the assembled radar system was placed on a platform with high vantage view of the intended target (located on the roof of Electrical Engineering building II of the National Taiwan Ocean University). The radar was set

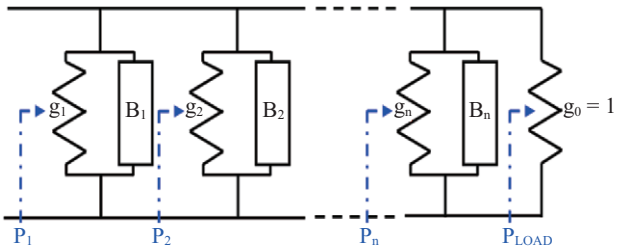

Fig. 3. Equivalent circuit of n elements edge-wall slotted waveguide array antenna.

to scan the Keelung Islet, which is about 4.48 km from the radar. It was also noticed that on the left of radar scanner, there is a newly constructed metal bridge connecting the main Taiwan Island to the nearby Peace Island. This huge structure, which is much closer to the radar (~1 km) will introduce large radar returns that may mask the intended radar signals of Keelung Islet. Nevertheless, this unintended obstruction will benefit the verification of the superior performance of the presently fabricated unit.

II. DESIGN CONSIDERATIONS

In this work, the design criteria are specified to be -33 dB SLL, cross-polarization < -33 dB, horizontal half-power beamwidth < 1.5°, and vertical half-power beamwidth < 22°. With the aid of 3D HFSS simulation software, the optimal flare half-angle φ = 30° is implemented to give the vertical half-power beamwidth < 22°. Similarly, the optimal slot spacing of 0.74λ is obtained to achieve the requirements of -33 dB SLL and horizontal half-power beamwidth < 1.5°. From the simulation, it is noted that a larger slot spacing will generate unwanted sidelobe in addition to the spreading of the main beam. On the other hand, a smaller slot spacing will result in an undesirably large deviation of the angle of the main beam from the antenna boresight. Deviation of the main beam from the antenna boresight over the operating frequency band is an intrinsic character of the presently studied traveling wave array antenna.

The edge-wall slotted waveguide array design begins with the determination of the radiating element with a given side lobe specification. The construction of the slotted structure for the generation of the desired excitation in each slot was implemented by the Taylor's aperture field distribution for edge-wall slotted waveguide array antenna with -33 dB SLL (Elliott, 2003). The linear radiating waveguide is an array of resonant shunt slots on the edge wall. A finite percentage of the input power is usually dissipated into the load and its equivalent circuit is represented in Fig. 3 (Jasik and Johnson, 1984; Gilbert and Volakis, 2007) with $Y_n = g_n + jB_n$, where Y_n, g_n, B_n are the equivalent admittance, conductance, and susceptance, respectively.

Determination of the resonant conductance plays an important role in waveguide array antenna design. The n^{th} slot resonant conductance g_n, can be written as (4):

$$g_n = \frac{P_n}{\left(1 - \sum_{i=1}^{n-1} P_i\right)} \tag{4}$$

where $\sum_{i=1}^{n-1} P_i = 1\text{-}P_L$. P_L is the power absorbed by the load at the end of the waveguide and P_i is the power radiated by the i^{th} slot. The slot parameters such as the inclined angle θ and depth d of the individual slot in the array must be selected so that a desired electric field distribution generated in the linear array can be matched to that of the Taylor's aperture field distribution.

The equivalent admittance Y_n can be analytically expressed in term of the scattering coefficient S_{11} as (Chernin, 1956):

$$Y_n = g_n + jB_n = \frac{-2S_{11}}{1 + S_{11}} \tag{5}$$

The equivalent admittance Y_n of the individual shunt slot with specified slot parameters θ and d was then simulated using HFSS simulation software. The effect of mutual coupling has been considered during the simulation process. Under resonance, the aperture's equivalent admittance is a real number, i.e. the imaginary part of the admittance or the susceptance is zero, *viz.*, $\mathrm{Im}(Y_n) = 0$ with n = 1, 2, 3….. In this study, we assume a quadratic relation of the form θ *or* $d = Ag_n^2 + Bg_n + C$ between the slots parameters θ and d with the n^{th} resonant conductance. The coefficients A, B, and C were determined by the least squared fit technique by fitting the quadratic polynomial to the simulated data points. The fitted relations were evaluated to be,

$$\theta = -900.7g_n^2 + 237.6g_n + 2.0 \quad \text{(degree)} \tag{6}$$

$$d = 114.1g_n^2 - 19.9g_n + 4.3 \quad \text{(mm)} \tag{7}$$

The variations of the inclined angle and depth d with the resonant conductance as given, respectively, by (6) and (7) are depicted in Fig. 4. The data points are plotted with the evaluated relations over the operating frequency. As shown, a considerable variation in the inclined angle and depth with the slot conductance is observed, changing from 1 degree at 4×10^{-4} *mho* for d = 4.45 mm to 20 degree at 2×10^{-1} *mho* for d = 3.45 mm. The numerically obtained relation (6) can be compared to the theoretical Stevenson's solution (Stevenson, 1948) for the slot conductance which can be expressed as (8):

$$g = \frac{30\lambda^3\lambda_g}{73\pi a^3 b}\left[\frac{\sin\theta\cos(\pi\lambda\sin\theta/2\lambda_g)}{1-(\lambda\sin\theta/\lambda_g)^2}\right]^2 \tag{8}$$

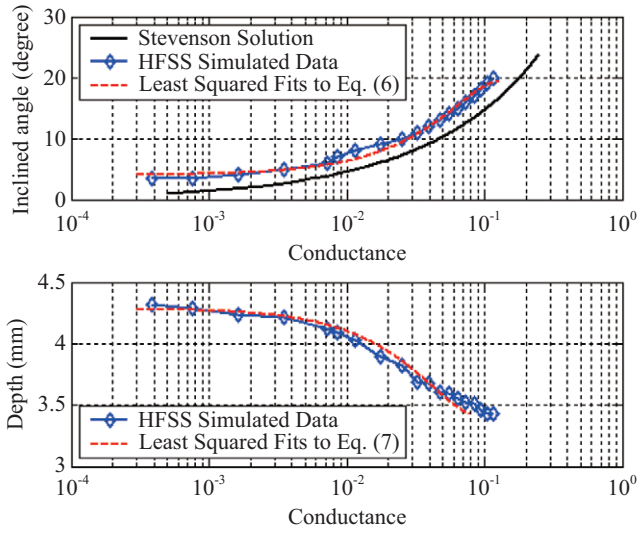

Fig. 4. Variation of inclined angle (top) and depth (bottom) with slot conductance.

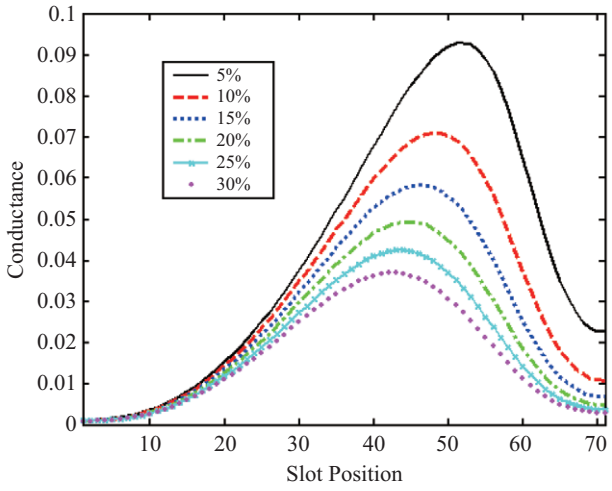

Fig. 5. Conductance distribution with the slot position for different percentage of the power dissipated into the load.

As seen on the top of Fig. 4, the two expressions agreed quite well with some deviation. The small discrepancy is most probably due to the assumption of perfectly conducting thin waveguide wall (Chang et al., 1996; Ando et al., 2007) and the absence of mutual coupling in Stevenson's calculation. Our present study on the influence of depth cut d across the broad side of the guide wall on the performance of the edge-wall slotted waveguide array antenna is of considerable interest to antenna engineers in view of the non-negligible variation of the slot's conductance on d. Furthermore, the semi-empirical relations as given by Eq. (6) and Eq. (7) also offer relatively simple design guidelines for antenna engineers. The specified percentage of the absorbed power by the load will affect the power distribution of the linear array (Milligan, 2005). The distribution of conductance for the linear slot array elements for Taylor's distribution with -33 dB SLL, corresponding respectively, to 5%, 10%, 15%, 20%, 25%, and 30% of the power being absorbed by the load is depicted in Fig. 5. It is important to design well matched load, otherwise, the reflected power will radiate an undesirable side lobe signal.

The technology of metal flare is selected in order to enhance the array antenna gain and generate radiation pattern with desirable beamwidth. It is found that the flare half-angle φ has a remarkable effect on the gain of the array antenna. Generally speaking, the total pattern equals the element pattern multiplied by the array factor (Koerner and Rogers, 2000; Glamazdin et al., 2001). For n-elements array antenna an approximate empirical formula for the gain in dB can be written as:

$$Gain \cong 10\log_{10}\frac{32400}{\theta_h\theta_v}$$

$$\cong Gain_{\text{single}} + 3\log_2 \text{n} + 3\log_2(\frac{180^\circ}{\phi}) \quad \text{(dB)} \qquad (9)$$

In (9), $Gain_{\text{single}}$ is the gain of a single slot, θ_h is the horizontal half-power beamwidth and θ_v is the vertical half-power beamwidth. In the present design, $Gain_{\text{single}}$~5 dB, n = 71, and with $\phi = 30°$ give a gain of ~31.2 dB which is comparable to the commercially available design for marine radar specification.

III. SIMULATION AND RESULTS

The traveling wave or resonant array can be designed to have the main beam at any angle with respect to the guide's edge-wall normal. Design considerations for the successful performance of the edge-wall slot array antenna have been described and the relevant characteristic parameters were analyzed. The characteristics of the calculated results of edge slots can be optimized by the measured reflection coefficients S_{11} according to (5). The results were then utilized to modify the resonant depths and inclined angles. As mentioned earlier, the theoretical aperture field distribution at the operating frequency f_0 based on Taylor's aperture distribution for a seventy-one radiating elements array with -33 dB SLL was designed (Elliott and Kurtz, 1978; Elliott, 1979). The presently studied antenna was designed having a conductance distribution with 5% of power absorbed by the load as depicted in Fig. 5. The three-dimensional (3D) and contour plot of the normalized radiation pattern of the edge-wall slotted waveguide antenna array with metal flare were measured in a near-field measurement chamber with a scanning distance equal to 3λ above the antenna array and shown in Figs. 6 and 7. The aperture field distribution profile along the slot array can then be derived from the 3λ near-field radiation pattern and shown in Fig. 8. As shown in Fig. 8, the good agreement of the measured aperture field distribution and the intended Taylor distribution indicates the well design of the fabricated antenna.

The simulation software 3D Ansoft's HFSS (Ansoft Software) is used to calculate the electromagnetic characteristics

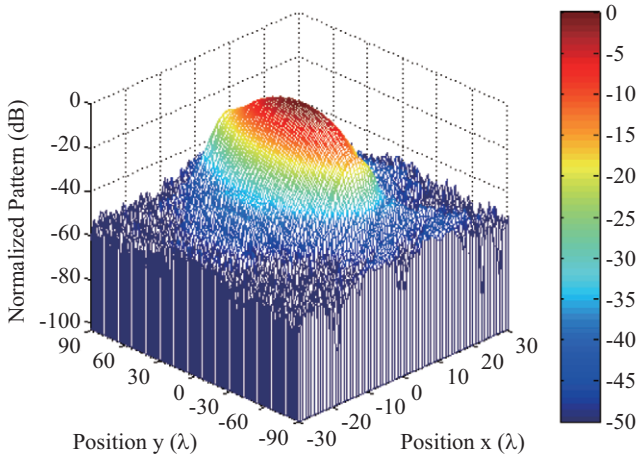

Fig. 6. Three-dimensional, normalized radiation pattern of the edge-wall slotted waveguide array antenna with metal flare. (Scanning distance equal to 3λ above the antenna array)

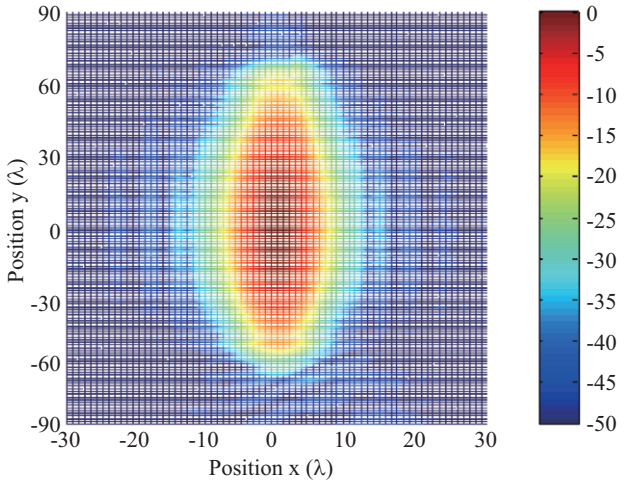

Fig. 7. Contour plot of the normalized radiation pattern of the edge-wall slotted waveguide array antenna with metal flare. (Scanning distance equal to 3λ above the antenna array)

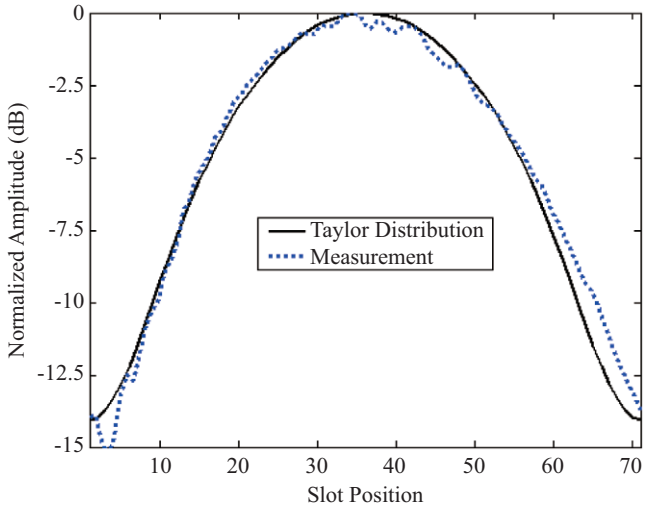

Fig. 8. Comparison of the theoretical and measured aperture field distribution of the normalized amplitude.

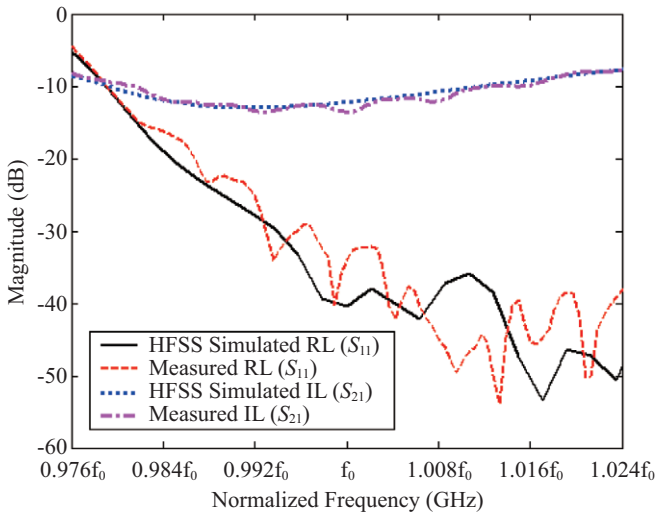

Fig. 9. Comparison of the simulated and measured reflection (S_{11}) and transmission coefficients (S_{21}).

(S_{11} and S_{21}) of the structure using the previously obtained resonant characteristic parameters θ and d. The results as illustrated in Fig. 9 show good agreement between the simulated and measured scattering coefficients. In Fig. 9, the magnitude of the measured and simulated return loss, S_{11}, is at least -13.6 dB over the designed frequency f_0. For the insertion loss S_{21}, the magnitude changes from -11.68 dB at $0.984f_0$ to -10.39 dB at $1.016f_0$ and an agreement to within ±1 dB can be achieved for the measured and simulated values. According to the measurements, the designed array antenna operates well with a bandwidth of 3.2% from $0.984f_0$ GHz to $1.016f_0$ GHz. The radiation efficiency as obtained from S_{21} is very close to the intended design of 95%.

The mechanical structure of the array antenna consists of precision machined aluminum component parts that are dip brazed into a hardy, lightweight assembly. Nevertheless, in order to construct the intended array antenna which can generate the desired radiation pattern, a highly skilled manufacturing process is necessary. The development of a variety of computer-aided technology, 3D electromagnetic simulation software, the CNC machine tool and a skilled welding technology must be established to accomplish the task.

The 3D radiation pattern of the edge-wall slotted waveguide array antenna with metal flare is shown in Fig. 10 which shows good radiation pattern and excellent performance for the fabricated antenna array. The larger the array antenna aperture, the smaller the antenna beamwidth will be in the plane along the array. The radiation pattern of the constructed seventy one slots gives a horizontal half-power beamwidth of 1.38° and a vertical half-power beamwidth of 21°. The performance conforms well to the designed specifications. It is known that the

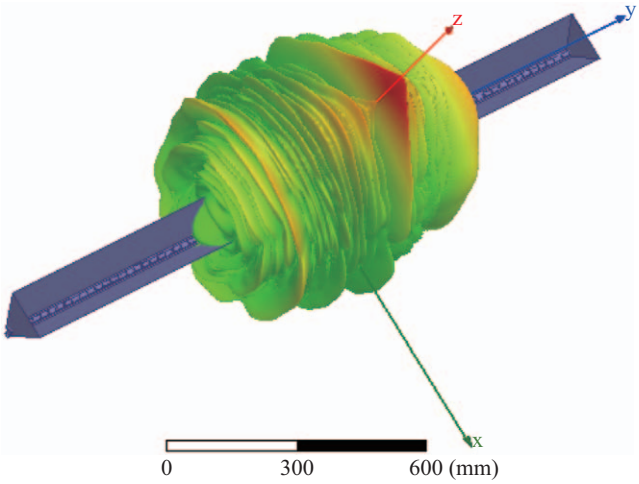

Fig. 10. 3D radiation pattern of the edge-wall slotted waveguide array antenna with metal flare (L × W × H = 1800 mm × 150 mm × 150 mm).

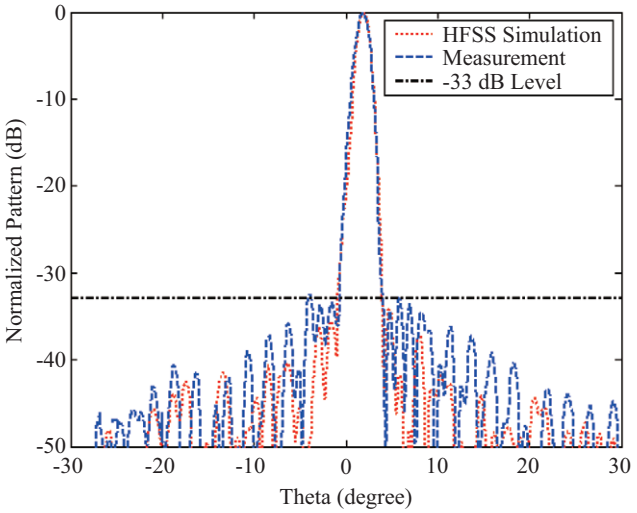

Fig. 11. Comparison of normalized measured and simulated Co-polarized far-field radiation pattern for the edge-wall slotted waveguide array antenna with metal flare.

edge-shunt slots may lead to non-negligible cross-polarization. In order to alleviate such problem, a suppressor consisting of a strip grating has been inserted in front of the antenna array. The width of the metal strip is ~ 0.01λ with a spacing of ~ λ/8. The far-field Co-polarized radiation patterns of the fabricated edge-wall slotted waveguide array antenna with and without the suppressor have been measured and together with the HFSS simulated results are illustrated in Figs. 10 and 11. Simulated 3D radiation pattern of the edge-wall slotted waveguide array antenna with metal flare is depicted in Fig. 10 showing the intended fan-beam pattern with ultralow SLL of less than -33 dB. In Fig. 11, both measured and simulated Co-polarized normalized radiation pattern of the edge-wall slotted waveguide array antenna with metal flare having a

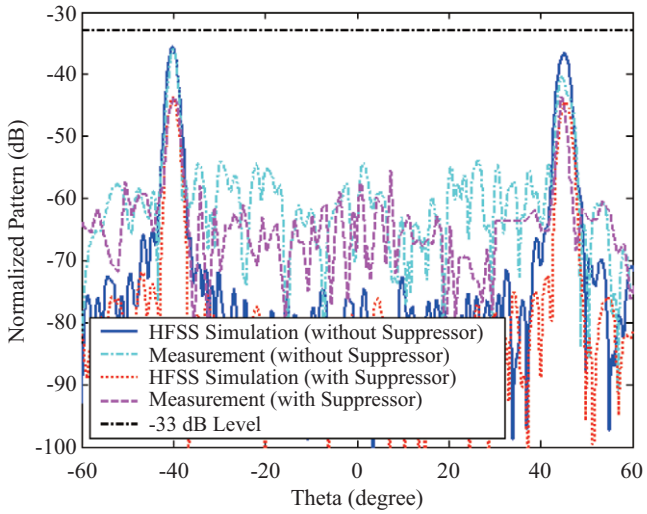

Fig. 12. Comparison of normalized measured and simulated Cross-polarized far-field radiation pattern with and without suppressor for the edge-wall slotted waveguide array antenna with metal flare.

-33 dB SLL with scanning range from -30° to 30° for center frequency corresponding to a position 2° off the broadside is illustrated. The results show excellent agreement between the simulated and measured Co-polarized far-field radiation patterns with SLL well within the -33 dB level. It is emphasized that for Co-polarization, the insertion of suppressor made little difference to the measured results and therefore only the measured results with suppressor inserted is included in Fig. 11. Fig. 12 depicts the measured and simulated Cross-polarized far-field radiation patterns for the fabricated unit. The scanning range is from -60° to 60° with respect to the center frequency. The measured results with and without the suppressor are included in Fig. 12 for comparison. From Fig. 12, it can be seen that inclusion of a suppressor can quench the Cross-polarized component by 8~10 dB. In any case, the cross-polarized component is small (less than the -33 dB SLL) compared to the Co-polarized counterpart. This result again indicated the well design of the antenna unit.

Radar detects targets by transmitting high frequency microwaves and then collecting some of those that are reflected from the targets. The direction of the target is determined by the direction in which the rotating radar antenna is pointing when it receives the reflected transmission. Plane Position Indicator (PPI) images from the experimental radar system were collected and shown in Figs. 13 and 14. Keelung Islet is a small island (4.48 km from radar scanner) located at 3.35 km northeast of the northern shore of Keelung, Taiwan and 4.9 km away from the Port of Keelung. The islet is made up of mostly multifaceted steep mountain terrain composed of andesite. As such, the effective radar cross section can be quite small due to the random scattering of the impinging radar waves from the faceted terrain. Nevertheless, as shown in Fig 13, the radar return from the islet is quite clear and the image showed

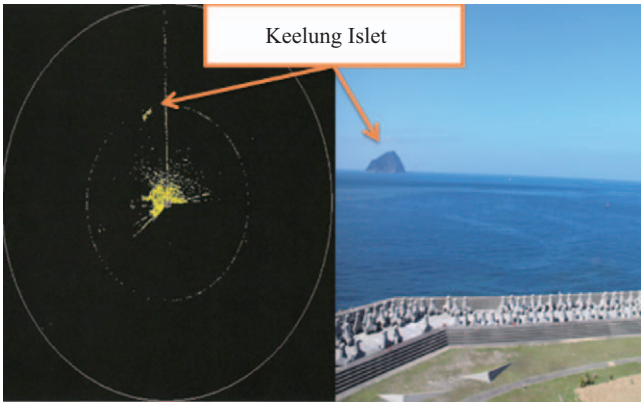

Fig. 13. PPI image of Keelung Islet.

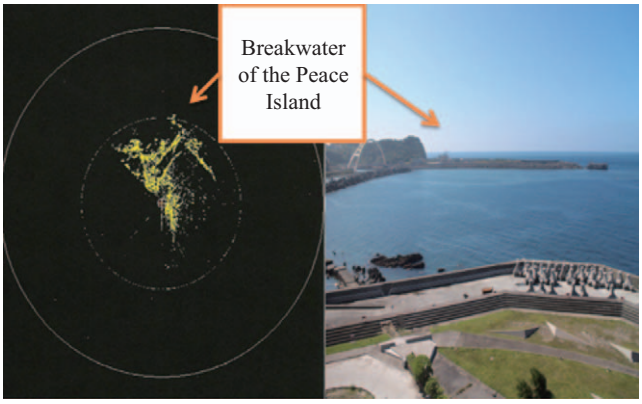

Fig. 14. PPI image of the metal bridge and the nearby breakwater.

no signal return (as a result of sidelobe effect) from the huge metal bridge. The clear radar display of Keelung Islet as shown in Fig. 13 showed the excellent performance of the ultralow sidelobes radiator unit. As a comparison, the strong radar return from the nearby metal bridge and the adjacent breakwater structure is illustrated in Fig. 14 with the radar scanner directly pointing at these structures.

IV. CONCLUSIONS

The radiation characteristics of an edge-wall slotted waveguide array antenna with the feature of ultralow SLL have been designed and tested. Metal flare was included to improve the antenna gain and a strip grating suppressor was also inserted to suppress the cross-polarized far-field radiation pattern. The single traveling wave array antenna has dimensions of 1800 mm × 150 mm × 150 mm and consists of seventy-one radiating elements with -33 dB SLL. The present design has considered a more realistic situation in which the finite waveguide wall thickness has been taken into consideration. The variation of the slot inclined angle and slot depth with the resonant conductance have been derived with a least squared quadratic curve fitting procedure.

The characteristics of the designed antenna array, including return loss, gain, and radiation pattern have been measured to verify the operating performance. Both simulated and measured results show that the slotted waveguide array antenna has low SLL with high gain. The good agreement between the simulated and measured results over a frequency range from $0.984f_0$ GHz to $1.016f_0$ GHz indicated the excellent design of the antenna array.

ACKNOWLEDGMENTS

The authors would like to thank Green Energy and Environment Research laboratories, Industrial Technology Research Institute (ITRI) for partial financial support in carrying out this research.

REFERENCES

Ando, M., J. Hirokawa, Y. Kazama and J. C. Young (2006). Full-wave optimization of Linear, Edge slot array with flare and choke for decreased vertical beamwidth and cross-polarization. IEEE Antennas and Propagation Society International Symposium and USNC/URSI National Radio Science Meeting, 2761-2764.

Ando, M., J. Hirokawa and J. C. Young (2007). Analysis of a rectangular waveguide, edge slot array with finite wall thickness. IEEE Transations on Antennas and Propagation 55(3), 812-819.

Ansoft Software Inc.. Ansoft simulator, version 12.0.

Balanis, C. E. (2005). Antenna Theory: Analysis and Design. John Wiley & Sons, New York.

Brown, C. and M. Howard (2004). Results of the electromagnetic investigations and assessments of marine radar, communications and positioning systems undertaken at the North Hoyle wind farm by QinetiQ and the maritime and coastguard agency. MCA and QinetiQ Ltd. UK.

Chang, D. C., P. Hsu, C. G. Jan and R. B. Wu (1996). Analysis of edge slots in rectangular waveguide with finite waveguide wall thickness. IEEE Transations on Antennas and Propagation 44(8), 1120-1126.

Chernin, M. (1956). Slot admittance data at Ka band. IRE Transations on Antennas and Propagation 4(4), 632-636.

Elliott, R. S. (1979). On the design of traveling-wave-fed longitudinal shunt slot arrays. IEEE Transations on Antennas and Propagation 27(5), 717-720.

Elliott, R. S. (2003). Antenna Theory and Design. Revised Edition. John Wiley & Sons, New York.

Elliott, R. S. and L. Kurtz (1978). The design of small slot arrays. IEEE Transations on Antennas and Propagation 26(2), 214-219.

Emmet, R. W., J. L. Hilburn, R. A. Kinney and F. H. Prestwood (2007). Frequency-scanned X-band waveguide array. IEEE Transations on Antennas and Propagation 20(4), 506-509.

Gilbert, Roland A. (chapter author) and John L. Volakis (editor) (2007). Antenna Engineering Handbook. Fourth Edition. McGraw-Hill, New York.

Glamazdin, V. V., M. P. Natarov, V. N. Skresanov and V. I. Tkachenko (2001). Waveguide longitudinal narrow wall slot radiating between bafflies. Matching analysis. Physics and Engineering of Millimeter and Sub-Millimeter Waves 2, 607-609.

Jasik, H. and R. C. Johnson (1984). Antenna Engineering Handbook. Second Edition. McGraw-Hill, New York.

Koerner, M. A. and R. L. Rogers (2000). Gain enhancement of a pyramidal horn using E- and H-plane metal baffles. IEEE Transations on Antennas and Propagation 48(4), 529-538.

Matthews, J. C. G., J. Pinto and C. Sarno (2009). Radar signature reduction of wind turbines through the application of stealth technology. European Conference on Antennas and Propagation, 3886-3890.

Milligan, T. A. (2005). Modern Antenna Design. Second Edition, John Wiley and Sons, New York.

Ramo, S., T. Van Duzer and J. R. Whinnery (1984). Fields and Waves in Communication Electronics. Second Edition, John Wiley and Sons, New York.

Skolnik, M. (2001). Introduction to Radar Systems. Third Edition. McGraw-Hill, New York.

Stevenson, A. F. (1948). Theory of slots in rectangular waveguide. Journal of Applied Physics 19(1), 24-38.

Yaghjian, A. D. (1986). An overview of near-field antenna measurements. IEEE Transations on Antennas and Propagation 34(1), 30-45.